Wheat drought assessment by remote sensing imagery using unmanned aerial vehicle

Wheat Drought Assessment by Remote Sensing Imagery Using Unmanned Aerial Vehicle

Jinya Su[1,2], Matthew Coombes[1], Cunjia Liu[1], Lei Guo[3], Wen-Hua Chen[1]

1. Department of Aeronautical and Automotive Engineering, Loughborough University, Loughborough LE11 3TU, U.K.
E-mail: J.Su2@lboro.ac.uk, M.J.Coombes@lboro.ac.uk, C.Liu5@lboro.ac.uk, W.Chen@lboro.ac.uk

2. Key Laboratory of Measurement and Control of Complex Systems of Engineering (Southeast University), Ministry of Education, China

3. School of Electrical Engineering and Automation, Beihang University, Beijing 100191, China. E-mail: lguo@buaa.edu.cn

Abstract: This work aims at evaluating the usability of remote sensing RGB imagery by an Unmanned Aerial Vehicle (UAV) in assessing wheat drought status. A UAV survey is conducted to collect high-resolution RGB imageries by using DJI S1000 for the experimental wheat fields of Gucheng town, Heibei Province, China. The soil moisture for different plots of the experimental filed is kept at an approximately constant level for the whole growing season in a well controlled environment, where field measurements are performed just after the UAV survey to obtain the soil water content for each plot. A machine learning based wheat drought assessment framework is proposed in this work. In the proposed framework, wheat pixels are first segmented from the soil background using the classical normalized excess green index (NExG). Rather than using pixel-wise classification, a pixel square of appropriate dimension is defined as the samples, based on which various features are extracted for the wheat pixels including statistical features and spectral index features. Different classification algorithms are experimented to identify a suitable one in terms of classification accuracy and computation time. It is discovered that Support Vector Machine with Gaussian kernel can obtain an accuracy over 90%, which demonstrates the usefulness of RGB imagery in wheat drought assessment.

Key Words: Classification, Remote sensing, UAV imagery, Wheat drought

1 Introduction

Water stress usually has adverse effects on plants such as closing stomata, up-taking less carbon dioxide, which inevitably diminish crop growth resulting in less biomass and yield [1]. In addition, water scarcity has become one of the top three global problems and China is a vast country with severe shortage of water. It is reported that agriculture takes 62.06% of fresh water for the arable land in the north part of China. Unfortunately, the current efficiency of irrigation in China is only about 52%, well below advanced countries which can achieve an efficiency of about 70%–80% of water usage. Therefore, there is an urgent need to optimize the irrigation scheduling so that irrigation efficiency can be improved, i.e. significantly reducing the water usage while meeting crop needs and maintaining crop productivity and yield [2]. It is evident that direct or indirect crop drought assessment is a prerequisite for optimizing irrigation strategy. Consequently, this work is focused on indirect wheat drought assessment.

Various crop drought monitoring approaches are available in the literature which can be broadly divided into direct ground measurement based approaches and indirect remote sensing based approaches. Ground measurement based approach is usually labour-intensive, time-consuming and with a high cost. This is because a large amount of sampling points need to be defined to cover a large area, and experimental test is required to determine the crop/soil water stress. As a result, there is a trend to adopt remote sensing technology to infer drought information extracted from spectral measurement of various cameras. For example, satellites equipped with multispectral camera can provide useful moisture information regarding the soil and crop, where shortwave infrared (SWIR) bands are directly related to water absorption [3, 4] and near-infrared band is also closely related to plant water status [5]. Although suitable for large area applications, it is also acknowledged that there are certain drawbacks for satellite based remote sensing [6], summarized as below

- The cost of satellite remote sensing is usually high;
- The spatial resolution of satellite imageries is usually low and can be easily affected by environment such as cloud;
- The revisit time of satellite is usually fixed and not flexible.

On the other hand, with user-defined spatial-temporal resolutions, low cost and flexibility, Unmanned Aerial Vehicle (UAV) based remote sensing is drawing increasing research interest, and has become an important complement for satellite or manned aircraft based remote sensing [7]. In this approach, different spectral cameras (e.g. RGB, multispectral, hyperspectral, thermal) can be installed on UAV for various applications including water stress assessment [8, 9].

This work is mainly focused on evaluating the usability of remote sensing RGB imagery by a small UAV of low altitude in assessing wheat drought status. In this work, the RGB camera is chosen mainly due to its low cost and simple data processing in comparison with multispectral and hyperspectral cameras. A UAV survey was performed by installing Sony NEX-7 camera on the commercial aircraft DJI S1000 to collect high-resolution RGB imageries, where the experimental wheat fields as detailed in Section 2.1 are chosen with different wheat plots being carried out different water treatments throughout the whole wheat growing seasons in a well controlled environment by using intelligent irrigation system and rain shelter. Field measurements are also performed just after the UAV survey to calculate the soil water

This work was supported by Science and Technology Facilities Council (STFC) under Newton fund with grant number ST/N006852/1 and the Newton Network+ NeWMap project. The first author is also financially supported by the Open Project Program of Ministry of Education Key Laboratory of Measurement and Control of CSE, under Grant MCCSE2017A01.

ratio for each wheat plot. As a result, a real UAV RGB imagery data with groundtruth soil water rate is obtained for wheat drought assessment.

Then a machine learning based wheat drought assessment framework is developed in this work, which are mainly composed of the following basic steps.

- Data collection: collect a series of high-resolution aerial imageries using the low altitude UAV-camera system, i.e. DJI S1000 with Sony NEX-7;
- Data pre-processing: pre-process UAV imageries to derive an orthomosaic image using Agisoft software and crop the region of interest;
- Wheat pixel segmentation: segment wheat pixels from background (e.g. road, soil and residue) using the classical normalized excess green index NExG; this is because there are no enough soil pixels in wheat fields under wet condition for data-driven analysis;
- Feature extraction and classifier training: define appropriate features for wheat pixels under different conditions, and train the classification model. In this work, rather than deploying pixel-wise classification, pixel squares of approximate dimension are treated as the samples, based on which different features are extracted including statistical features and spectral index features.
- Deploy the learnt classifier to the field of interest to generate the classification map.

Based on the developed framework, it was discovered that a classification accuracy over 90% can be achieved using the classical SVM classifier with Gaussian kernel in discriminating wheat pixel under wet and dry plots, which demonstrates the usefulness of UAV RGB imagery of low altitude in assessing wheat drought status. The trained classifier is also applied to the whole region to derive a classification map including wheat under wet condition, wheat under dry condition and background. The main contribution of the work is to develop a complete machine learning based wheat drought assessment framework and validate its effectiveness using real experimental data. And the main conclusion is that UAV RGB imageries of low altitude is useful in assessing wheat drought status. It is noted that an extended version of the work is given in [10].

The remaining part of the paper is organized as follows. Section 2 introduces the study site, filed measurements and UAV-camera systems. In Section 3, the machine learning based wheat drought assessment framework is elaborated. In Section 4, the experimental results are presented. Section 5 concludes the paper with future work discussion.

2 Materials

In this section, materials for the UAV survey are given including study site, field measurements and UAV-camera systems for airborne imageries.

2.1 Study site: wheat filed

The study was carried out in the wheat field of the Gucheng Ecological-Meteorological Integrated Observation Experiment Station, Chinese Academy of Meteorological Sciences, which is located at the east of Gucheng town, Dingxing county in Hebei Province, China ($39^o08'N$, $115^o40'E$, elevation of 15.2m). There is totally 42 wheat plots for soil water content experiments, which are well separated from each other using a special design. The crop under investigation is winter wheat.

2.2 Field measurements of soil water rate

The experimental wheat field is designed in such a way that soil moisture of each plot is kept at an approximately constant level for the whole growing season in a well controlled environment by using rain shelter and intelligent irrigation system. The raw soil samples of each plot are collected on 10th, April, 2017 at depth of 10 centimetre and 20 centimetre respectively to attenuate uncertainties. After raw soil samples were weighted using Electronic Balances BS-423S, they were then processed using Drying Ovens DHG-9245A to remove water and weighted again so that soil water rates were calculated by the ratio, where the final soil water rate was calculated by taking the average. The soil water rates can generally be divided into two classes (e.g. high and low), and consequently the wheat plots are termed wet wheat plot and dry wheat plot respectively depending on the corresponding soil water rate.

2.3 UAV-camera systems and airborne imageries

In this work, the commercial aircraft DJI S1000 was used as the platform of low altitude UAV-camera system and the Sony NEX-7 is chosen as the RGB camera. During the flight, the camera was fixed on a gimbal, pointing vertically downwards.

The airborne campaigns were conducted at about 20 meters above the ground on 09th, April, 2017 and the spatial resolution of the final orthomosaic image was 4.54 mm/pix. A laptop installed with Ground Controlling Station (GCS) software was used to monitor and control the autonomous UAV flight through telemetry radio. The cameras were triggered so that an overlap up to 75 % of imageries could be obtained. Then 36 UAV imageries were stitched using the commercial software PhotoScan (Agisoft, Russia) so that an orthomosaic image (covering an area of 3540 m^2) could be generated.

The RGB image for the Region Of Interest (ROI) is cropped from the orthomosaic image and shown in Fig 1, where 18 different plots are analysed including 11 wet plots and 6 dry plots. For the same of simplicity, the left-column plots are termed west 1 to west 6 from top to bottom, similarly, the middle-column plot i and right-column plot i are termed Middle i and East i respectively.

3 Machine learning based wheat drought assessment framework

There is no explicit relationship between UAV imageries and soil water ratio and so the implicit relationship has to be worked out using data-driven approaches [11]. Consequently, in this paper, a machine learning based framework was proposed to evaluate the usefulness of UAV remote sensing imagery of low altitude (in particular RGB imageries) in wheat drought assessment. The complete flowchart of the proposed framework is displayed in Fig. 2, which mainly comprises of image preparation and pre-processing, wheat segmentation, training samples construction including feature extraction, classifier training and classification. Some key elements of the developed framework are detailed in the

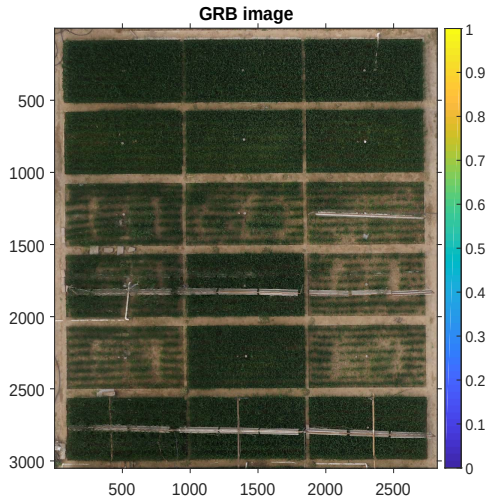

Fig. 1: RGB image of FoI from the orthomosaic image.

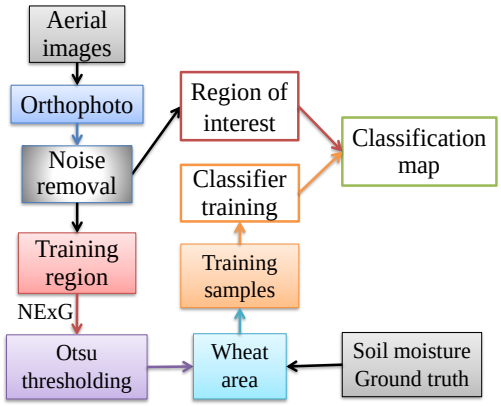

Fig. 2: Flowchart of the proposed machine learning based wheat drought assessment framework.

following subsections.

3.1 Image pre-processing

With a series of aerial imageries, the commercial software PhotoScan (Agisoft, Russia) is first adopted to generate an orthomosaic image. Then the orthomosaic image is processed using Gaussian blur filter to reduce the effects of random noises. On this basis, the region of interest can be cropped from the orthomosaic image for the following wheat pixel segmentation and further processing.

3.2 Wheat segmentation

Directly assessing soil moisture is highly desirable, however, this is hard for wheat at a late growing stage (i.e. with a high canopy cover). This is mainly because the soil pixels at high canopy cover regions are very limited as can be seen from Fig 1. Consequently, this work instead works on wheat pixels. As a result, it is necessary to separate wheat pixels from soil and residue background.

This is usually achieved by inspecting the differences in spectral reflectance between vegetation and soil pixels. Green plants usually show relatively low values in Red and Blue channels with a peak in Green spectral band in comparison to background pixels [12]. However, initial studies demonstrate that non-normalised RGB values were not suitable for this task, since they are directly proportional to the total light reflected from a surface and therefore highly sensitive to illuminating intensity [13]. Instead different colour based vegetation indices are frequently used in the literature. To ease understanding of the notations, throughout this paper, Red, Green and Blue denote the digit number of different RGB channels either in the range of $[0, 255]$ or $[0, 1]$; while red, green, blue denote the normalized values (or chromaticity conversion) of Red, Green and Blue by dividing Red, Green and Blue by $(Red + Green + Blue)$.

There exist a number of vegetation indices to segment crop from background, such as normalized excess green index $NExG = 2g - r - b$ [14], normalized difference index $NDI = (Green - Red)/(Green + Red)$ [13], Excess Green minus Excess Red $ExG - ExR$ [15], where ExR denotes excess red $ExR = 1.3R - G$ [16] among many others. In this work, the NExG is adopted due to its fine performance via trial & error experiments; NExG represents the difference of the divergence of both red from green and blue from green.

To remove background pixels from RGB image including road, and soil above wheat field, it is necessary to define an appropriate threshold for the one dimensional NExG index distribution. In this paper, the well known Otsu's thresholding method [17] is adopted, which finds the optimal threshold by maximizing the weighted sum of between-class variances. The derived threshold is 0.345 using Otsu's algorithm and the wheat segmentation result is shown in Fig 3.

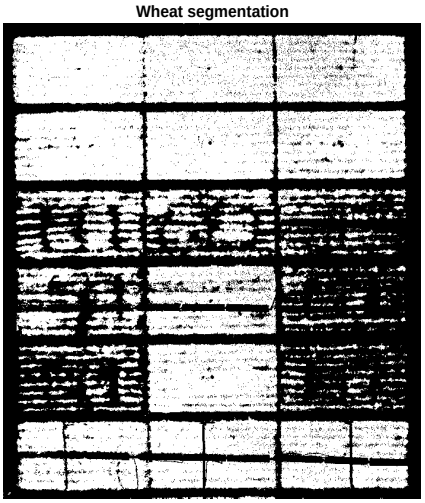

Fig. 3: Wheat segmentation using Otsu's algorithm: wheat (white pixels), background (black pixels).

Remark: In this work, spectral index is adopted to segment wheat pixel from background due to its simplicity and generality. More advanced algorithms can also be adopted to achieve this wheat segmentation task such as various clustering algorithms based on various spectral features.

3.3 Samples and feature extraction

Machine learning applications highly rely on training samples. Consequently, in this section, the training samples along with the corresponding features for classification model construction are detailed.

3.3.1 Samples

In machine learning applications, a vital step is to define appropriate training samples, from which corresponding features can be extracted for classification model contribution. In remote sensing for precision agriculture, there are generally a large number of pixels and so pixel-wise classification is usually time-consuming in both training and classification. In addition, in pixel-wise classification, the features are usually limited to pixel values and more representative features (such as texture feature, statistical features) can not be defined. To improve the effectiveness and efficiency of the classification algorithms, in this work, instead of conducting pixel-wise classification a sample is defined by a pixel square of dimension $k \times k$ with k being a pre-defined value. Consequently, the volume of data can be substantially reduced since k^2 pixels are treated as one sample.

The ground truth data for soil water rate is given in Section 2.2, however, it is for each plot rather than specific wheat pixels or pixel square as aforementioned. In this paper, the training samples under wet soil plot and dry soil plot are chosen in the following steps.

Algorithm 1: Steps to derive samples

(1) Plot selection: pixels in West 1&2 are chosen for wet wheat, and the pixels in West 3 and Middle 3 are for dry wheat.;

(2) Pixel square: the aforementioned regions are gridded into pixel square of dimension $k \times k$;

(3) Non-wheat pixel removal: only pixel squares with wheat pixel proportion over 20% is kept as a wheat sample.

(4) Sample label: the remaining pixel squares after non-wheat pixel removal are labelled using the label for the plots.

Following the steps in Algorithm 1, a labelled training dataset is obtained for classification algorithm training and selection.

3.3.2 Feature extraction

With the samples defined in Section 3.3.1, we further define appropriate features extracted from pixel squares to maximally represent the properties of the samples. In this work, various types of features are defined for the wheat pixels in the pixel squares including statistical features and special index features. The statistical features include mean, variance, range, standard derivation, skewness and entropy for each RGB band. Three special index features are also considered including $GoR = Green/Red$, $NExG = 2g - r - b$ and $NDI = (Green - Red)/(Green + Red)$; with loss of generality only the mean values of the aforementioned spectral indices within the pixel squares are considered. There are totally 21 features.

Generally speaking, feature selection can be further adopted to select the most representative features to reduce the computation load or even improve the classification performance [20]. However, in this work all 21 features are directly used in classification model. This is because on the one hand the number of features is not high and on the other hand the training and testing samples are also not large due to pixel square rather than pixel in sample construction.

3.4 Classifier training

With labelled training samples for wet wheat and dry wheat, the next step is to train a classifier with which given a new sample its class label can be determined. Different classification algorithms are available in the literature. There is a built-in App termed "classificationLearner" in Matlab, which can quickly evaluate the performance of different classification algorithms including Decision tree, Discriminant analysis, Logistic regression, Support Vector Machine (SVM), K-Nearest Neighbors (KNN) among many others. In this work, this App is adopted to train different types of classification models so that the most suitable one in terms of classification accuracy and computation time can be identified. In this process, the five-fold cross validation is adopted to evaluate the classification performance. Then the learnt classification model can be applied to the whole ROI for real application.

4 Results and discussions

In this part, experimental validation of the proposed framework for wheat drought assessment using remote sensing RGB imagery of low altitude is conducted.

As discussed in Section 3.4, different classification algorithms are first compared using five-fold cross-validation in the "classificationLearner" App. The classification performance (with 3314 training samples) along with computation time using Matlab 2017a on Windows computer using Intel Core i5-3570 CPU@3.4GHz with RAM 8GB are summarized in Table 3. Considering the classification accuracy and computation time concurrently, SVM with Gaussian kernel is adopted in this paper, which can achieve a satisfying performance while taking a reasonable training time.

Table 1: Classifier performance comparison

Algorithm	Accuracy	Time (sec)
Complex tree	86%	1.98
Medium tree	88.4%	0.56
Logistic Regression	90.0%	3.58
SVM (Quadratic)	90.5%	10.2
SVM (Gaussian)	90.3%	1.57
KNN (Cosine)	89.0%	0.52

Second, the classification map for the ROI using SVM with Gaussian kernel is performed. In this process, the whole imagery is first gridded into the corresponding pixel squares using Algorithm 1 so that features can be extracted. The classification time is 0.27 sec, which is very fast. The classification results are displayed in Fig. 4. To make the result more interpretable, the corresponding groundtruth map for different plots is also displayed.

It can be visually seen from Fig 4 that

(1) The ratio of yellow pixels is high in dry plots and low in wet plots, so the classification results are very positive;

(2) Most of the classification errors for wet wheat plot appear at the boundary of the wheat plot; this is mainly because some soil pixels and wheat pixels are put into one pixel square in creating testing dataset.

Overall, it can be concluded that remote sensing RGB imageries obtained by using an UAV of a low altitude can provide valuable information for wheat drought assessment.

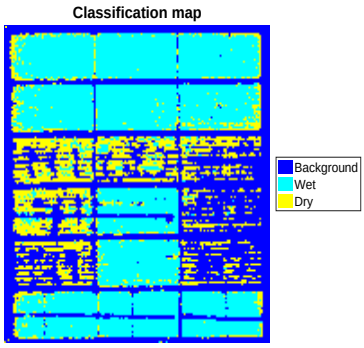

Fig. 4: Classification map with background pixels (blue), wet wheat pixels (cyan) and dry wheat pixels (yellow).

And the main reason is that wheat grew in dry soil condition will reflect different RGB reflectance from the wheat grew in wet soil condition.

5 Conclusions and future work

This paper is mainly focused on evaluating the usefulness of UAV RGB imagery on wheat drought assessment. An experiment has been carefully designed for wheat drought comparison by keeping the soil moisture of wheat fields at an almost constant level (i.e. wet field and dry field). RGB imageries are collected by using DJI-S1000 with Sony NEX-7 camera. A machine learning based framework for wheat drought assessment has been proposed by integrating various techniques such as image processing, feature engineering and classification. It is shown that the developed framework can achieve an accuracy of over 90% in discriminating wet wheat and dry wheat. This is only an initial study, where future works are summarized in the following aspects.

(i) To perform a more reliable wheat drought assessment, other bands including NIR, Short-wavelength (SWIR) for water absorption, and Mid-wavelength (MWIR) for temperature should also be considered. Then Multi-spectral images are generated, which can provide a better discriminating ability;

(ii) Experiments should be further designed so that wheat under different levels of drought can be analysed so that a regression analysis can be conducted between special indices and soil water content.

(iii) At an early stage with smaller value of canopy cover, it would be of interest to verify whether UAV imagery can be used to assess the soil drought.

References

[1] H. Nilsson, "Remote sensing and image analysis in plant pathology," *Annual Review of Phytopathology*, vol. 33, no. 1, pp. 489–528, 1995.

[2] X.-P. Deng, L. Shan, H. Zhang, and N. C. Turner, "Improving agricultural water use efficiency in arid and semiarid areas of china," *Agricultural water management*, vol. 80, no. 1, pp. 23–40, 2006.

[3] B.-C. Gao, "Ndwia normalized difference water index for remote sensing of vegetation liquid water from space," *Remote sensing of environment*, vol. 58, no. 3, pp. 257–266, 1996.

[4] R. Oltra-Carrió, F. Baup, S. Fabre, R. Fieuzal, and X. Briottet, "Improvement of soil moisture retrieval from hyperspectral vnir-swir data using clay content information: From laboratory to field experiments," *Remote Sensing*, vol. 7, no. 3, pp. 3184–3205, 2015.

[5] J. Peñuelas, I. Filella, C. Biel, L. Serrano, and R. Save, "The reflectance at the 950–970 nm region as an indicator of plant water status," *International journal of remote sensing*, vol. 14, no. 10, pp. 1887–1905, 1993.

[6] T. Zhang, J. Su, C. Liu, W.-H. Chen, H. Liu, and G. Liu, "Band selection in sentinel-2 satellite for agriculture applications," in *Automation and Computing (ICAC), 2017 23rd International Conference on*, pp. 1–6, IEEE, 2017.

[7] C. Zhang and J. M. Kovacs, "The application of small unmanned aerial systems for precision agriculture: a review," *Precision agriculture*, vol. 13, no. 6, pp. 693–712, 2012.

[8] J. Baluja, M. P. Diago, P. Balda, R. Zorer, F. Meggio, F. Morales, and J. Tardaguila, "Assessment of vineyard water status variability by thermal and multispectral imagery using an unmanned aerial vehicle (uav)," *Irrigation Science*, vol. 30, no. 6, pp. 511–522, 2012.

[9] T. Zhao, B. Stark, Y. Chen, A. L. Ray, and D. Doll, "Challenges in water stress quantification using small unmanned aerial system (suas): Lessons from a growing season of almond," *Journal of Intelligent & Robotic Systems*, vol. 88, no. 2-4, pp. 721–735, 2017.

[10] J. Su, M. Coombes, C. Liu, L. Guo, S. Fang, and W.-H. Chen, "Machine learning based crop drought mapping system by using uav remote sensing imageries," *under review*, 2018.

[11] D. Yi, J. Su, C. Liu, and W.-H. Chen, "Personalized driver workload inference by learning from vehicle related measurements," *IEEE Transactions on Systems, Man, and Cybernetics: Systems*, 2017.

[12] C. Lin, "A support vector machine embedded weed identification system," 2010.

[13] A. Perez, F. Lopez, J. Benlloch, and S. Christensen, "Colour and shape analysis techniques for weed detection in cereal fields," *Computers and electronics in agriculture*, vol. 25, no. 3, pp. 197–212, 2000.

[14] D. Woebbecke, G. Meyer, K. Von Bargen, and D. Mortensen, "Color indices for weed identification under various soil, residue, and lighting conditions," *Transactions of the ASAE*, vol. 38, no. 1, pp. 259–269, 1995.

[15] G. E. Meyer and J. C. Neto, "Verification of color vegetation indices for automated crop imaging applications," *Computers and electronics in agriculture*, vol. 63, no. 2, pp. 282–293, 2008.

[16] G. E. Meyer, T. W. Hindman, and K. Lakshmi, "Machine vision detection parameters for plant species identification," in *SPIE, Bellingham, WA*, 1998.

[17] N. Otsu, "A threshold selection method from gray-level histograms," *IEEE transactions on systems, man, and cybernetics*, vol. 9, no. 1, pp. 62–66, 1979.

[18] P. Steduto, T. C. Hsiao, D. Raes, and E. Fereres, "Aquacropthe fao crop model to simulate yield response to water: I. concepts and underlying principles," *Agronomy Journal*, vol. 101, no. 3, pp. 426–437, 2009.

[19] D. Kim and J. Kaluarachchi, "Validating fao aquacrop using landsat images and regional crop information," *Agricultural Water Management*, vol. 149, pp. 143–155, 2015.

[20] J. Su, D. Yi, C. Liu, L. Guo, and W.-H. Chen, "Dimension reduction aided hyperspectral image classification with a small-sized training dataset: Experimental comparisons," *Sensors*, vol. 17, no. 12, p. 2726, 2017.